JCAMECH

Vol. 50, No. 1, June 2019, pp 165-173
DOI: 10.22059/jcamech.2019.278376.372

A Theoretical study of steady MHD mixed convection heat transfer flow for a horizontal circular cylinder embedded in a micropolar casson fluid with thermal radiation

Hani Qadan [a,*], *Hamzeh T. Alkasasbe* [b] *and* Nusayba M. Yaseen [c], *Mohammed Z. Swalmeh*[c,], *Shaima IbrahIm ALKhalafat*[c]

[a] *Faculty Engineering, Department of Civil Engineering, Al-Balqa Applied University, Amman-Jordan*
[b] *Department of Mathematics, Faculty of Science, Ajloun National University, P.O. Box 43, Ajloun 26810, Jordan*
[c] *Faculty of art and science, Aqaba University of Technology, Aqaba-Jordan*

ARTICLE INFO

Article history:
Received: 25 March 2019
Accepted: 16 April 2019

Keywords:
Casson Fluid_1
Horizontal Circular Cylinder_2
Magnetohydrodynamic (MHD)_3
Micropolar Fluid-4
Numerical Solution-5
Radiation-6

ABSTRACT

In this study, an investigation is carried out for laminar steady mixed 2D magnetohydrodynamic (MHD) flow of micropolar Casson fluid with thermal radiation over a horizontal circular cylinder with constant surface temperature. In the present study, an investigation is carried out on the effects of physical parameters on Casson fluid non dimensional numbers. The governing nonlinear partial differential equations and the controlling boundary conditions are derived for this case study. Furthermore, these equations are solved numerically using finite difference technique known as Keller Box Method (KBM). The effects of non-dimensional governing parameters, namely Casson parameter, mixed convection parameter, magnetic parameter, radiation parameter on the Nusselt number and local friction coefficient, as well as temperature, velocity and angular velocity are discussed and shown graphically. It is noticed that the local skin friction and the local Nasselt number has decrement behaviors when increasing the values the Casson parameter. But the opposite happens when the mixed convection parameter λ increase. It is found that the results in this study are in good agreement with previous studies. This proves that calculations using KBM method and the chosen step size are accurate enough for this type of problems.

1. Introduction

In material and chemical engineering processing, the non-Newtonian fluid flow branches, has different types of fluids like viscoelastic, couple stress, power low, and Casson. Casson fluid has many applications in practice because it is better than the general visco-plastic model in fitting the rheological data (Pushpalatha, Sugunamma et al.) . Casson fluid is also reflects the shear thickening property. On the other hand, Casson fluid shows the behavior of Newtonian property when the shear stress increases to a level much higher than the yield stress.

In 1959, Casson forecast flow behavior of pigment-oil suspensions of printing ink (Casson 1959). The heat flow of a Casson fluid over an impulsive motion of the plate using the homotopy method has been studied by Mustafa et al, (Mustafa, Hayat et al.). Mukhopadhyay et al. (Mukhopadhyay, Bhattacharyya et al.) reported that, the exact solution of forced convection boundary layer Casson fluid flow toward a linearly stretching surface with transpiration effects. The velocity and thermal slip conditions on laminar boundary layer heat transfer flow of a Casson fluid past a

* Corresponding author. Tel.: 00962785112491; e-mail: hani_qadan@yahoo.com

vertical plate, have been studied by Subba et al (Subba Rao, Ramachandra Prasad et al.). Mahdy and Ahmad (Mahdy and Ahmed) studied the effect of magneto-hydrodynamic on mixed convection boundary flow of an in compressible Casson fluid in the stagnation point of an impulsively rotation sphere. Nagrndra et al.(Nagendra, Amanulla et al.) presented the convective boundary layer flow of Casson nano-fluid from an isothermal sphere surface. Mehmood et al (Mehmood, Mehmood et al.) studied in detail the micro-polar Casson fluid on mixed convection flow induced by a stretching sheet. Shchzad et al. (Shehzad, Hayat et al.) discussed the various chemical reaction effects on MHD flow of Casson fluid over porous stretching sheet. The exact solution for unsteady MHD free convection flow of a Casson fluid on oscillating plate was studied by Khalid et al. (Khalid, Khan et al.). The most widely food substances examples of Casson fluid are jelly, tomato sauce, honey, soup, concentrated fruit juices. Many researchers such as Abolbashari et al. (Abolbashari, Freidoonimehr et al.), Animasaun (Animasaun), Mukhopadhyay and Vajravelu (Mukhopadhyay, Mondal et al.), Prasad et al. (Prasad, Rao et al.) have shown interest in studying the characteristics of Casson fluid in various physical situations. Many other investigators on Casson fluid, the reader may refer to, like Qasim and Noreen (Qasim and Noreen); Husanan et al., Haq et al (Haq, Nadeem et al.), and Alkasabsbeh et al. (Alkasasbeh, Salleh et al. 2014).

A micropolar fluid comprise of rigid, randomly distributed particles in glutinous medium. This kind of fluids has many practical applications in blood, foodstuffs, polymers, plasma, drilling oil, and gas wells. This fluid contains nonsymmetrical stress tensors. Many researchers worked on this type of fluid, such as Erigen (Eringen 1966)who worked on the theoretical explanation of micropolar fluids. The theory of Lukaszewicz (Lukaszewicz 1999)described the micropolar fluid, that the flow lies in the extension of the constituent equation for a Newtonian fluid so that more complex fluids such as liquid crystal, particle suspensions, animal blood, lubrication and turbulent shear flows. Furthermore, he proposed the logical and significant overview of the Navier-Strokes model, covering both in theory and applications, many more phenomena than the classical one. Amiran et al (Ariman, Turk et al. 1973), explained in detail the applications of the fluids experiencing micro rotation at the particle level. Khonsari and Brewer (Khonsari and Brewe 1994) investigated the effects of viscous dissipation on lubrication characteristics of micropolar fluids. Moreover, they reported that the existence microstructure (based on micropolar theory) tends to enhance the load carrying capacity and friction coefficient.

Many investigators carried out studies of the boundary layer flow on a horizontal circular cylinder. Blasius (1908) (Blasius 1908) solved the momentum equation of forced convection boundary layer flow. Merkin (Merkin 1976) was the first to find the exact solution on an isothermal horizontal cylinder with constant wall temperature by considering the free convection boundary layer. Moreover, a numerical method to solve free convection boundary layer flow on an isothermal horizontal was developed by Ingham (Ingham 1978). Furthermore, The mixed convection boundary-layer flow of a micropolar fluid over a horizontal was investigated by Nazar et al. (Nazar, Amin et al. 2003). The magneto-hydrodynamic (MHD) free convection flow and heat transfer of non-Newtonian tangent hyperbolic fluid from horizontal circular cylinder with convection boundary conditions, were studied by Gaffar et al. (Gaffar, Prasad et al.).

Based on the above studies, the main target of the present study is to investigate the effect of (MHD) on mixed convection boundary layer flow over a horizontal circular cylinder in micropolar Casson fluid with thermal radiation subjected to constant wall temperature. The boundary-layer equations are solved numerically via efficient implicit finite-difference scheme known as the Keller-box method, as displayed by Cebeci et al.(Cebeci and Bradshaw). The effects of the Casson parameter, the radiation parameter, magnetic parameter and mixed convection parameter on the local heat transfer, local skin friction, temperature, around the circular cylinder are discussed and explained in the tables and figures. For comparison purposes, the results for $M = 0, R=0, \beta \to \infty$ and $K = 0$ (regular Newtonian fluid) and Pr = 7 are computed, and they show excellent agreement with those obtained by (Nazar, Amin et al. 2003).

Malik et.al investigated the boundary layer flow of nanofluid over a vertical exponentially stretching cylinder(Malik, Naseer et al.). Venkantesan et.al studied the mathematical analysis of Casson fluid for blood rheology in sterosed narrow arteries(Venkatesan, Sankar et al.). Gul et.al carriedout a research on the thin film flow analysis of MHD third grade fluid on a vertical belt with no slip boundary conditions(Gul and Ullah). Abid et.al investigated the magnetic hydrodynamic flow of unsteady second grade fluid between two vertical plates with oscilating boundary conditions(Abid, Islam et al.).

There are many industerial applications of non-Newtonian fluids like ketchup, custered, salt solutions, molten polymers, starch suspensions, blood, and shampoo. This research will serve to know the physical properties and their relationships and consequently improve quality of production industy.

2. Mathematical Modeling

Consider the steady, laminar, two-dimensional, viscous, incompressible, buoyancy-driven mixed convection heat transfer flow from a horizontal circular cylinder embedded in a micropolar Casson fluid. Figure 1.a shows the flow model and a physical coordinate system. The $\bar{x}-$coordinate is measured along the circumference of the horizontal cylinder from the lowest point and the $\bar{y}-$coordinate is measured normal to the surface, with a denoting the radius of the horizontal cylinder. $\bar{x}/a$ is the angle of the $\bar{y}-$axis with respect to the vertical $0 \le \bar{x}/a \le \pi$. The gravitational acceleration, g acts downwards. Both the horizontal cylinder and the fluid have maintained the surface of the cylinder temperature, T_w with $T_w > T_\infty$ for a heated cylinder (assisting flow) and $T_w < T_\infty$ for a cooled cylinder (opposing flow).

The constitutive relationship of an incompressible Casson fluid flow, conducted by (Mukhopadhyay, Bhattacharyya et al. 2013).

$$\tau_{ij} = \begin{cases} 2\left(\mu_B + p_y\sqrt{2\pi}\right)e_{ij} & \pi > \pi_c, \\ 2\left(\mu_B + p_y\sqrt{2\pi_c}\right)e_{ij} & \pi < \pi_c, \end{cases}$$

Such that $\pi = e_{ij}e_{ij}$, e_{ij} is the (i, j)-th component of the deformation rate, μ_B π_c and p_y are the plastic dynamic viscosity of the non-Newtonian fluid, the critical value of this product based on the non-Newtonian model and the yield stress of the fluid, respectively.

The boundary layer approximations, the continuity, momentum, micro-rotation and energy equations, respectively can be displayed as (Mohammad 2015):

$$\frac{\partial}{\partial \bar{x}}(\bar{u}) + \frac{\partial}{\partial \bar{y}}(\bar{v}) = 0, \tag{1}$$

$$\begin{aligned} \bar{u}\frac{\partial \bar{u}}{\partial \bar{x}} + \bar{v}\frac{\partial \bar{u}}{\partial \bar{y}} &= \bar{u}_e\frac{d\bar{u}_e}{d\bar{x}} + \left(\frac{\mu+\kappa}{\rho}\right)\left(1+\frac{1}{\beta}\right)\frac{\partial^2 \bar{u}}{\partial \bar{y}^2} \\ &+ gB(T-T_\infty)\sin\left(\frac{\bar{x}}{a}\right) + \frac{\kappa}{\rho}\frac{\partial \bar{H}}{\partial \bar{y}} - \frac{\sigma {B_0}^2}{\rho}\bar{u} \end{aligned} \tag{2}$$

$$\rho j\left(\bar{u}\frac{\partial \bar{H}}{\partial \bar{x}}+\bar{v}\frac{\partial \bar{H}}{\partial \bar{y}}\right)=-\kappa\left(2\bar{H}+\frac{\partial \bar{u}}{\partial \bar{y}}\right)+\phi\frac{\partial^2 \bar{H}}{\partial \bar{y}^2}, \tag{3}$$

$$\bar{u}\frac{\partial T}{\partial \bar{x}}+\bar{v}\frac{\partial T}{\partial \bar{y}}=\alpha\frac{\partial^2 T}{\partial \bar{y}^2}-\frac{1}{\rho c_\rho}\frac{\partial q_r}{\partial \bar{y}} \tag{4}$$

Where the boundary conditions which is defined by (Swalmeh, Alkasasbeh et al. 2018),

$$\bar{u}=\bar{v}=0,\ T=T_w,\ \bar{H}=-\frac{1}{2}\frac{\partial \bar{u}}{\partial \bar{y}}\ \text{as}\ \bar{y}=0,$$

$$\bar{u}\to 0,\ T\to T_\infty,\ H\to 0,\ \text{as}\ \bar{y}\to\infty, \tag{5}$$

where $\bar{u}$ and $\bar{v}$ are the velocity components along the $\bar{x}$ and $\bar{y}$ directions, respectively, $\bar{H}$, $\bar{u}_e(\bar{x})=U_\infty \sin\left(\frac{\bar{x}}{a}\right)$, κ, T, g, k , σ, α, B, B_0^2, ν, μ, ρ, $j=a^2/\sqrt{Gr}$, $\beta=\mu_B\sqrt{2\pi_c}/p_y$ and $\varphi=(\mu+(\kappa/2))j$ are the angular velocity of micropolar fluid, the local free-stream velocity, the vortex viscosity, the local temperature, the gravity acceleration, the thermal, conductivity, the electric conductivity, the thermal diffusivity, the thermal expansion coefficient, magnetic field strength, the kinematic viscosity, the dynamic viscosity, the fluid density, the microinertia density, the parameter of the Casson fluid, and the spin gradient viscosity, respectively.

.

We introduce now the following non-dimensional variables,

$$x=\frac{\bar{x}}{a},\quad y=\mathrm{Re}^{1/2}\left(\frac{\bar{y}}{a}\right),$$

$$u=\frac{\bar{u}}{U_\infty},\quad v=\mathrm{Re}^{1/2}\left(\frac{\bar{v}}{U_\infty}\right), \tag{6}$$

$$H=\left(\frac{a}{U_\infty}\right)\mathrm{Re}^{1/2}\,\bar{H},\ \theta=\frac{T-T_\infty}{T_w-T_\infty},$$

where $\mathrm{Re}=U_\infty\frac{a}{\nu}$, is the Reynolds number (Nazar, Amin et al. 2003) and $Gr=\frac{gB(T_w-T_\infty)a^3}{\nu^2}$, is the Grashof number.

Using the Rosseland approximation for radiation, the radioactive heat flux is simplified as (Bataller (2008) (Cortell Bataller 2008))

$$q_r=\frac{4\sigma'}{3k'}\frac{\partial T^4}{\partial \bar{y}} \tag{7}$$

Where σ' and k' are the Stefan-Boltzmann constant and the mean absorption coefficient respectively. We assume that the temperature difference within the flow through the micopolar fluid such as the term T^4 may be expressed as a linear function of temperature. Hence, expanding T^4 in Taylor series about T_w and neglecting higher order items, we get

$$T^4\cong 4T_\infty^3T-3T_\infty^4 \tag{8}$$

Substituting variables (6)-(8) into equations (1)-(4) we obtain the following non-dimensional equations of the problem under consideration.

$$\frac{\partial}{\partial x}(u)+\frac{\partial}{\partial y}(v)=0 \tag{9}$$

$$u\frac{\partial u}{\partial x}+v\frac{\partial u}{\partial y}=u_e\frac{du_e}{dx}+\left(1+K+\frac{1}{\beta}\right)\frac{\partial^2 u}{\partial y^2}$$
$$+\lambda\theta\sin x+-Mu+K\frac{\partial H}{\partial y} \tag{10}$$

$$u\frac{\partial H}{\partial x}+v\frac{\partial H}{\partial y}=-K\left(2H+\frac{\partial u}{\partial y}\right)+\left(1+\frac{K}{2}\right)\frac{\partial^2 H}{\partial y^2}, \tag{11}$$

$$u\frac{\partial \theta}{\partial x}+v\frac{\partial \theta}{\partial y}=\frac{1}{\mathrm{Pr}}\left(1+\frac{4}{3}R\right)\frac{\partial^2 \theta}{\partial y^2}, \tag{12}$$

The boundary conditions (5) become

$$u=v=0,\ \theta=1,\ H=-\frac{1}{2}\frac{\partial u}{\partial y}\ \text{at}\ y=0$$

$$u\to u_e(x)\ \ \theta\to 0,\ H\to 0\ \text{as}\ y\to\infty \tag{13}$$

Where K, Pr, M, R and λ are the micropolar parameter, the Prandtl number, the magnetic parameter, the radiation parameter, the mixed convection parameter, respectively, which are given by:

$$K=\kappa/\mu\ ,$$
$$\mathrm{Pr}=\nu/\alpha\ ,M=\sigma B_0^2a/\rho U_\infty, \tag{14}$$
$$R=\alpha k^*\rho c_\rho/4\sigma^*T_\infty^3,\ \lambda=\frac{Gr}{\mathrm{Re}^2}.$$

with $Gr=gB(T_w-T_\infty)a^3/\nu^2$ is the Grashof number. Also worth mentioning that $\lambda>0$ corresponds to the assisting flow (heated cylinder), $\lambda<0$ corresponds to the opposing flow (cooled cylinder) and $\lambda=0$ corresponds to the forced convection flow.

To solve the system of equations (9) to (12), subjected to the boundary conditions (13), we assume the following variables:

$$\psi=xf(x.y),\ \theta=\theta(x,y),\ H=xh(x,y), \tag{15}$$

Where ψ is the stream function defined as

$$u=\frac{\partial \psi}{\partial y}\ \text{and}\ v=-\frac{\partial \psi}{\partial x}, \tag{16}$$

which satisfies the continuity equation (9). Thus, equations (10) to (12) become

$$\left(1+K+\frac{1}{\beta}\right)\frac{\partial^3 f}{\partial y^3}+f\frac{\partial^2 f}{\partial y^2}-\left(\frac{\partial f}{\partial y}\right)^2+\lambda\frac{\sin x}{x}\theta-M\frac{\partial f}{\partial y}$$
$$+\frac{\sin x\cos x}{x}+K\frac{\partial h}{\partial y}=x\left(\frac{\partial f}{\partial y}\frac{\partial^2 f}{\partial x\partial y}-\frac{\partial f}{\partial x}\frac{\partial^2 f}{\partial y^2}\right) \tag{17}$$

$$\left(1+\frac{K}{2}\right)\frac{\partial^2 h}{\partial y^2}+f\frac{\partial h}{\partial y}-\frac{\partial f}{\partial y}h$$
$$-K\left(2h+\frac{\partial^2 f}{\partial y^2}\right)=x\left(\frac{\partial f}{\partial y}\frac{\partial h}{\partial x}-\frac{\partial f}{\partial x}\frac{\partial h}{\partial y}\right) \tag{18}$$

$$\frac{1}{\mathrm{Pr}}\left(1+\frac{4}{3}R\right)\frac{\partial^2 \theta}{\partial y^2}+f\frac{\partial \theta}{\partial y}=x\left(\frac{\partial f}{\partial y}\frac{\partial \theta}{\partial x}-\frac{\partial f}{\partial x}\frac{\partial \theta}{\partial y}\right) \tag{19}$$

Subject to the boundary conditions

$$f=\frac{\partial f}{\partial y}=0,\ \ \theta=1,\ h=-\frac{1}{2}\frac{\partial^2 f}{\partial y^2}\ \ \text{at y=0}$$

$$\frac{\partial f}{\partial y}\to\frac{\sin x}{x},\ \ \theta\to 0,\ h\to 0\ \text{as}\ y\to\infty \tag{20}$$

It can be noticed that at the lower stagnation point of the cylinder $(x\approx 0)$, equations (17) to (19) reduce to the following ordinary differential equations:

$$\left(1+K+\frac{1}{\beta}\right)f'''+2ff''-f'^2+\lambda\theta-Mf'+Kh'+\frac{9}{4}=0, \quad (21)$$

$$\left(1+\frac{K}{2}\right)h''+2fh'-f'h-K(2h+f'')=0 \quad (22)$$

$$\frac{1}{\Pr}\left(1+\frac{4}{3}R\right)\theta''+f\theta'=0. \quad (23)$$

and the boundary conditions (21) become

$$f(0)=f'(0)=0,\ \theta(0)=1,\ h(0)=-\frac{1}{2}f''(0),$$
$$f'\to 1,\ \theta\to 0,\ h\to 0 \text{ as } y\to\infty \quad (24)$$

where primes denote differentiation with respect to y.

The physical quantities of interest in this problem are the local skin friction coefficient, C_f and the

local Nusselt number Nu which are defend by (Alkasasbeh 2018)

$$C_f=\frac{a}{U_\infty}\mathrm{Re}^{-1/2}\left(\mu+\frac{\kappa}{2}+\frac{P_y}{\sqrt{2\pi_c}}\right)\left(\frac{\partial\bar{u}}{\partial\bar{y}}\right)_{\bar{y}=0},$$
$$Nu=\frac{a}{k(T_f-T_\infty)}\mathrm{Re}^{-1/2}\left(\frac{\partial\bar{T}}{\partial\bar{y}}\right)_{\bar{y}=0} \quad (25)$$

Using the non-dimensional variables (8)-(10) and the boundary conditions (15) the local skin friction coefficient C_f and the local Nusselt number Nu are

$$C_f=\left(1+\frac{K}{2}+\frac{1}{\beta}\right)x\left(\frac{\partial^2 f}{\partial y^2}\right)_{y=o},$$
$$Nu=-\left(1+\frac{4}{3}R\right)\left(\frac{\partial\theta}{\partial y}\right)_{y=o}. \quad (26)$$

3. Results and discussion

Equations (17) - (19), subject to the boundary conditions. (20) have been solved numerically using an efficient implicit finite-difference scheme known as the Keller-box method with Newton's linearization technique as considered by Cebeci and Bradshaw [27].The results are shown in deferent figures for the effects of different parameters such as the magnetic parameter M, the radiation parameter R, the Casson parameter β, the mixed convection parameter λ and the micro-rotation parameter K on the local skin friction C_f, the local Nusselt number Nu and temperature profiles $\theta(0,y)$. The solutions of nonlinear partial differential equations start at the lower stagnation point of the horizontal circular cylinder $x\approx 0$, up to $x = 2\pi/3$, around of the Circumference of a circular cylinder with initial profiles as given by the equations (21) to (23), with initial condition (25) and step size Δy=0.02,and Δx=0.005 are used in software MATLAB(as shown in Figure 1.b). In Tables 1 and 2 present the comparison values between our results and the results reported by Nazar et al. (Nazar, Amin et al. 2003) (values between brackets) at Pr = 7, K = 0, M = 0, R = 0 and $\beta\to\infty$, (regular Newtonian fluid) for various values of λ. It is found that comparison is an excellent and good agreement. This proves that the numerical method used for the calculation (KBM) and the chosen step size is accurate enough for this type of problems.

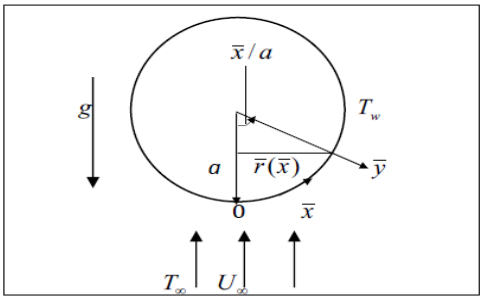

a

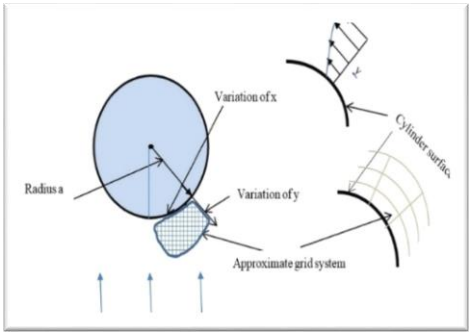

b

Figure. 1. a: Physical model and coordinate system
b: Coordinate and grid system for Physical model.

Table 1: Comparison of numerical values for local Nusselt number Nu at Pr = 0.7, K = 0, M = 0, R = 0 and $\beta\to\infty$, (Newtonian fluid), for viscous value of x with previously published results.

λ	-4	-3	-2	-1	-0.5	0.0	0.74	0.75
x								
	0.6518	0.7094	0.7516	0.7858	0.8009	0.8149	0.8342	0.8344
	(0.6534)	(0.7108)	(0.7529)	(0.7870)	(0.8021)	(0.8162)	(0.8354)	(0.8357)
30°		0.6499	0.7026	0.7421	0.7589	0.7743	0.7952	07955
		(0.6507)	(0.7027)	(0.7422)	(0.7591)	(0.7746)	(0.7955)	(0.7958)
60°			0.5333	0.6069	0.6321	0.6536	0.6810	0.6827
			(0.5309)	(0.6055)	(0.6309)	(0.6525)	(0.6800)	(0.6803)
90°					0.3835	0.4425	0.4941	0.4968
					(0.3796)	(0.4398)	(0.4920)	(0.4926)
120°								0. 1688
								(0.1276)

Table 2: Comparison of numerical values for local skin friction coefficient C_f at Pr = 0.7, K = 0, M = 0, R = 0 and $\beta \to \infty$, (Newtonian fluid), for viscous value of *x* with previously published results

λ	-4	-3	-2	-1	-0.5	0.0	0.74	0.75
x								
0°	0.0000	0.0000	0.0000	0.0000	0.0000	0.0000	0.0000	0.0000
	(0.0000)	(0.0000)	(0.0000)	(0.0000)	(0.0000)	(0.0000)	(0.0000)	(0.0000)
30°		0.4033	0.6747	0.9131	1.0246	1.1321	1.2852	1.2878
		(0.4024)	(0.6718)	(0.9098)	(1.0211)	(1.1284)	(1.2813)	(1.2833)
60°			0.5399	1.0965	1.3347	1.5580	1.8660	1.8770
			(0.5295)	(1.0866)	(1.3246)	(1.5477)	(1.8580)	(1.8621)
90°					0.4972	0.9296	1.4346	1.4638
					(0.4813)	(0.9154)	(1.4289)	(1.4352)
120°								0.0427
								(0.0380)

Comparison of the local skin friction and local Nusselt number with various values of the parameters such as the magnetic parameter M, the Casson parameter β, the mixed convection parameter λ and the radiation parameter R are given in figures 2 to 9 for the two micro-rotation parameter values (K = 2 , K = 5, and K=7).

Figures 2 and 3 shows the effect of the Casson parameter β on the local Nusselt number and the local skin friction. It is found that the local Nusselt number and the local skin friction decrease as increase the Casson parameter β .This is due to that high values of Casson parameter fluids are thick fluids (i.e. high values of plastic dynamic viscosity). Hence it has high shear stress values which results high values of Nusselt number and local skin friction.

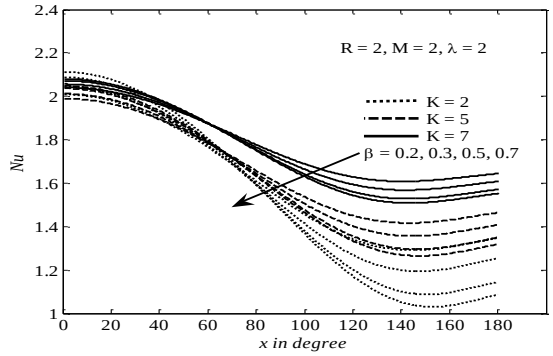

Figure2: Variation of the local Nusselt number Nu for different values of *x* and Casson parameter constant β .

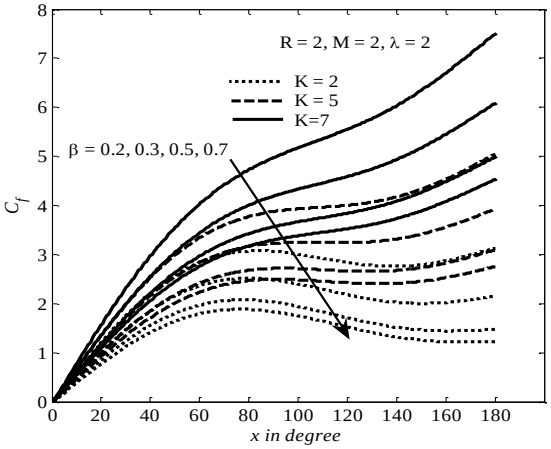

Figure 3: Variation of the local skin friction for different values of *x* and Casson parameter β .

Figure 4 and 5 display the effect of the radiation parameter R on the local Nusselt number and the local skin friction. We notice that an increase in radiation parameter R, the local Nusselt number and the local skin friction increase. This is due to increase in temperature difference and consequently increase in local skin friction and Nusselt number.

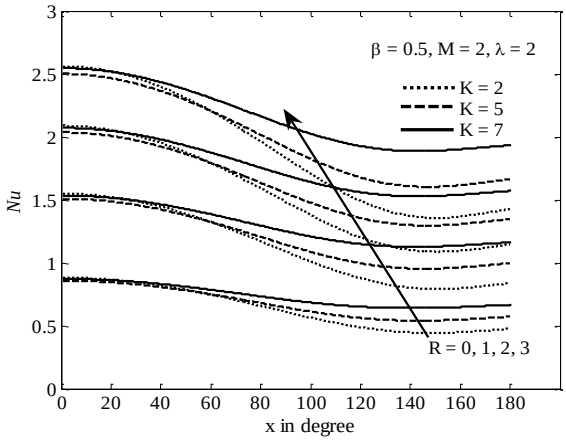

Figure 4: Variation of the local Nusselt number Nu for different values of *x* and Radiation parameter R.

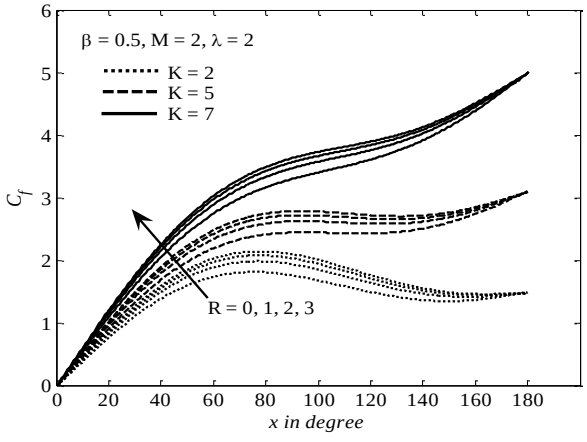

Figure5: Variation of the local skin friction C_f for different values of *x* and Radiation parameter R.

Figure 6 and 7 illustrate the influence of the magnetic parameter M on the local Nusselt number and the local skin friction, respectively. It is noticed from these figures that an increase of the magnetic parameter leads to decreases on both the local Nusselt number and the local skin friction. The increase in the thermal

expansion coefficient which increase the Grashof number and hence decrease the local skin friction and Nusselt number.

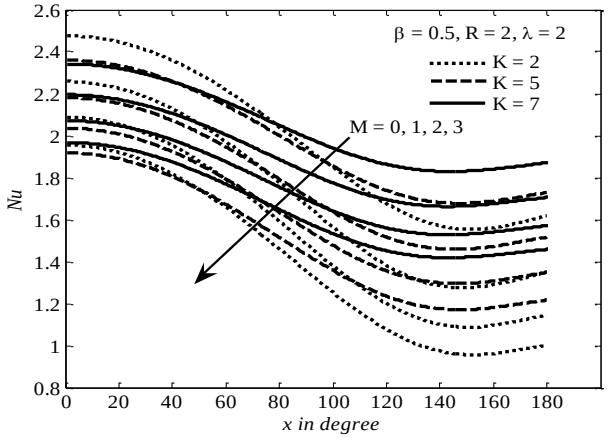

Figure 6: Variation of the local Nusselt number Nu for different values of *x* and magnetic parameter R

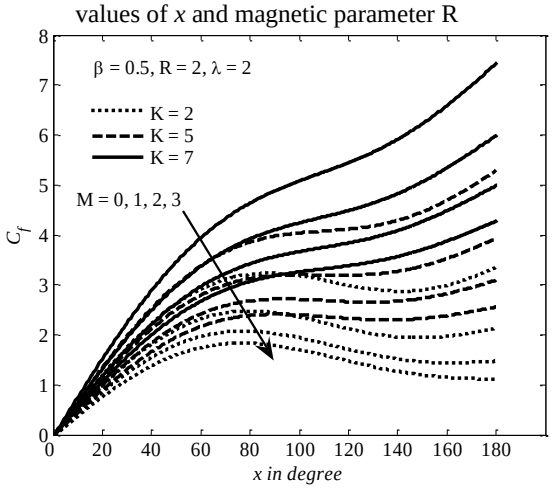

Figure 7: Variation of the local skin friction C_f for different values of *x* and magnetic parameter R

Figure 8 and 9 indicate the effect of the mixed convection parameter in the local Nusselt number and the local skin friction. It is seen that when the mixed convection parameter λ increase, the rate values of the local Nusselt number and the local skin friction number increase. Increasing the values of the values of mixed convection parameter cuase the dcrease the values of Renold number and consequently increase the values of local skin friction and Nusselt number.

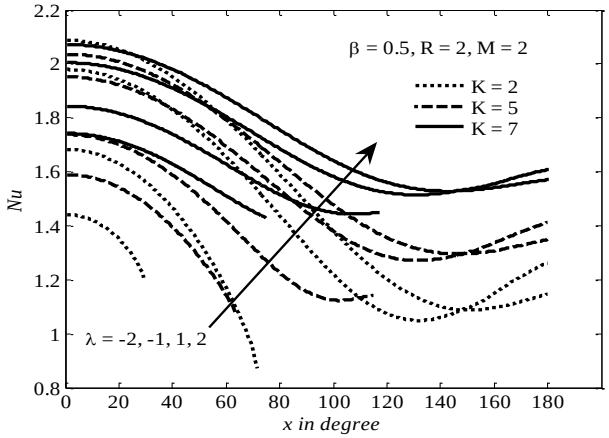

Figure 8: Variation of the local Nusselt number Nu for different values of *x* and mixed convection parameter λ

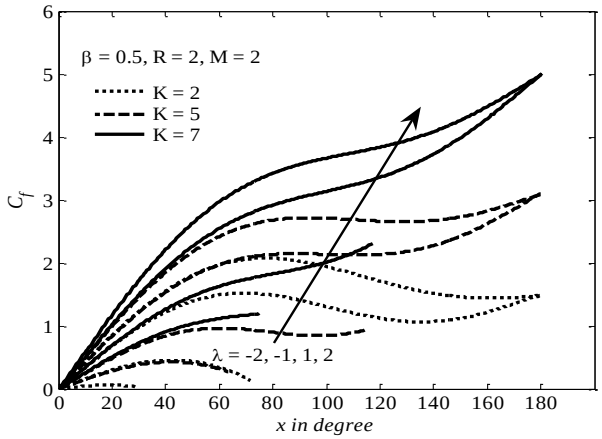

Figure 9: Variation of the local skin friction C_f for different values of *x* and mixed convection parameter

The effect of different parameters on the temperature profiles are depicted in Figures 10 to 13. We noticed that the temperature increases as the Casson parameter β decreases, the mixed convection parameter λ increases and the Radiation parameter R increases. While the Magnetic parameter M Shows increasing on the values of temperature profile by its increment. Low values of Casson parameter cause increase the temperature rate due to low viscosity of the fluid. Moreover, for values of mixed convection parameter result low values of Grashof number and hence low values of thermal expansion coefficient then low values of temperature rate.

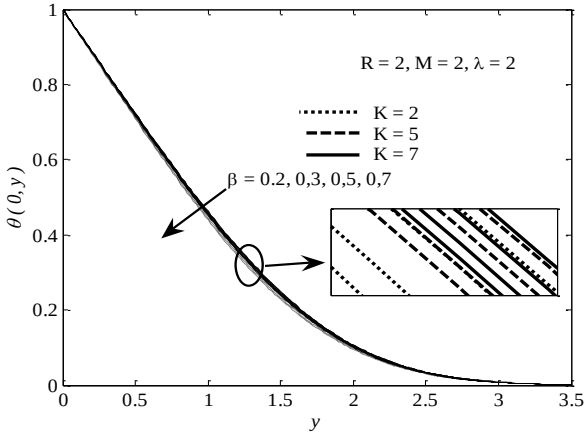

Figure 10: Influence of the temperature profiles for different values of *x* and Casson parameter β .

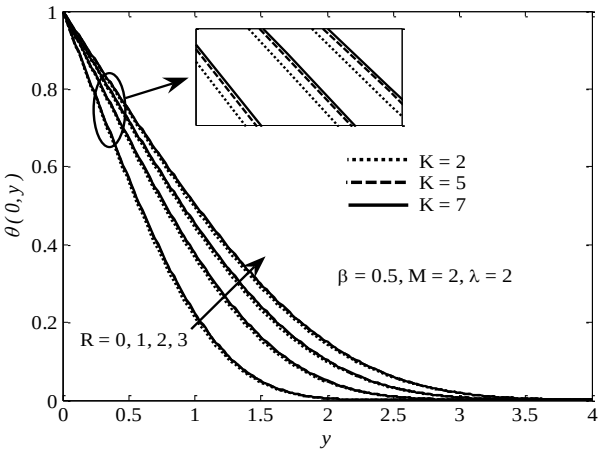

Figure 11: Influence of the temperature profiles for different values of *x* and radiation parameter R

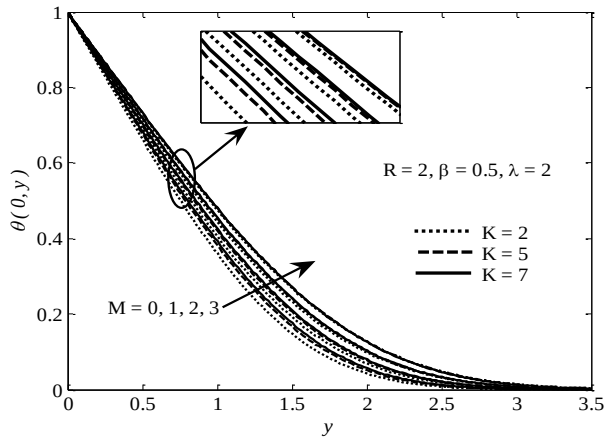

Figure 12: Influence of the temperature profiles for different values of *x* and magnetic parameter M

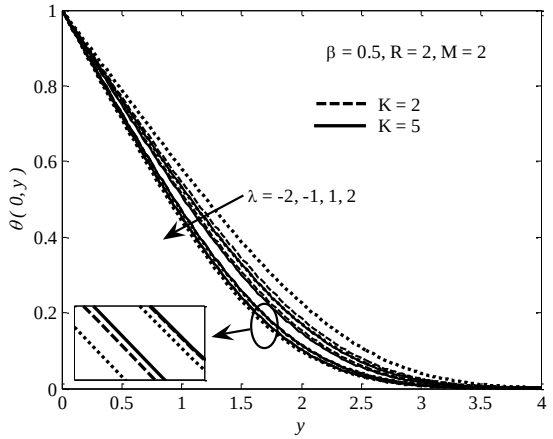

Figure 13: Influence of the temperature profiles for different values of *x* and mixed convection parameter λ

Finally, the changing of the micro-rotation parameter K for a higher value (from K=2 to K=5) on this study reflects on higher and stronger relationships between all previously discussed target parameters (R, M, λ, β). The curves elevated up on most graphs when K got the values of 5, higher difference and elevation is clearly shown or seen in Figures 3, 5, 7 and 9. Figures: 2, 4, 6 and 8 show a noticeable behaviour on the curves of K parameter; by moving the target parameter the curves going to intersect at certain points. The behaviour of higher K curve acts as strong decrement before the intersection point and higher increment after it. We can see also the intersection point is the same on both figures 2 and 4 while it tends to move to the right on figures 6 and 8.

4. Conclusions

In this paper, we have studied the problem of (MHD) mixed convection boundary layer flow over a horizontal circular cylinder immersed in a Casson fluid with constant wall temperature. We have looked into the effects of Casson parameter β (0.2, 0.3, 0.5, and 0.7), radiation parameter R (0, 1, 2, and 3), the magnetic parameter M (0, 1, 2, and 3) and mixed convection parameter λ (-2, -1, 1, 2), on the flow and heat transfer characteristics for micro rotation K (2, 5, 7). The partial differential equations were solved numerically via the Keller-Box Method (BKM) starting from stagnation point x=0 to x=2π/3 with step size Δ*y*=0.02, and Δ*x*=0.005 using MATLAB. From the output results and analysis, we have the following physical conclusions:

i. The local Nusselt number (with maximum value 2.15 at angle equal to zero and minimum value of 1.01 at angle equal to 150 degrees) decrease with different values of angle *x* when the values the Casson parameter β (0.2, 0.3, 0.5, and 0.7), increases for micro rotation parameter K (2, 5, and 7), convection parameter R=2, magnetic parameter M= 2 and convection parameter λ =2. It is noted that at an angle equal to 60 degrees for all Casson parameter values and micro rotation parameter the values of Nusselt number are the same (1.7).

ii. The local skin friction coefficient decrease with different values of *x* when the value the Casson parameter β (0.2, 0.3, 0.5, and 0.7) increases. It starts from zero at angle equal to zero and increasing positively in nonlinear way, and change curvature after angle equal to 80 degrees. For small values of micro rotation parameter, the local skin friction coefficient decreases at angles greater than 80 degrees. This scenario is repeated with the radiation parameter R (0, 1, 2, 3), magnetic parameter M for values of (0, 1,2, 3), and mix convection parameter λ (-2, -1, 1, 2)

iii. Nusselt number has maximum value (2.5) at x=0 and minimum value of (1.8) for radiation parameter R=3. On the other hand it has maximum value of (0.8) and minimum value of (0.6) for radiation parameter R=0. This scenario is repeated with the parameter M for values of (0, 1,2, 3)

iv. The rate of local Nusselt number and the local skin friction has a positive relationship with both radiation parameter R and mixed convection number λ with increase the values of micro-rotation parameter K.

v. The temperature profile increment depends on the increment of radiation parameter R and magnetic parameter M. On the other hand, the temperature profile decrease as increase the mixed convection number λ and the Casson parameter β .

Nomenclature

g	Acceleration due to gravity $\left[m \cdot s^{-2}\right]$
Gr	Grashof number
B_0^2	magnetic field strength
β	The parameter of the Casson fluid
M	magnetic parameter
R	radiation parameter
Re	Reynolds number
j	Micro-inertia density $\left[m^2\right]$
K	Micro-rotation parameter
k	Base fluid thermal conductivity $\left[W \cdot m^{-1} \cdot K^{-1}\right]$
$\bar{H}$	Angular velocity $\left[m \cdot s^{-1}\right]$
Pr	Prandtl number
T	Temperature of the fluid $\left[K\right]$
T_w	Wall temperature $\left[K\right]$

T_∞ Ambient temperature $\left[K\right]$

u x-component of velocity $\left[m \cdot s^{-1}\right]$

v y-component of velocity $\left[m \cdot s^{-1}\right]$

Greek symbols

λ Mixed convection parameter

α Thermal diffusivity $\left[m^2 \cdot s^{-1}\right]$

κ Vortex viscosity $\left[kg \cdot m^{-1} \cdot s^{-1}\right]$

μ Fluid dynamic viscosity $\left[kg \cdot m^{-1} \cdot s^{-1}\right]$

ρ Fluid density $\left[kg \cdot m^{-3}\right]$

B Fluid thermal expansion coefficient $\left[K^{-1}\right]$

ϕ Spin gradient viscosity $\left[kg \cdot m \cdot s^{-1}\right]$

ψ Stream function

θ Dimensionless temp.

w Condition at wall

∞ Condition at infinity

References

[1] Abid, S., S. Islam, et al. "Magnetic hydrodynamic flow of unsteady second grade fluid between two vertical plates with oscillating boundary conditions." J. Appl. Environ. Biol. Sci 4(01): 0-01.

[2] Abolbashari, M. H., N. Freidoonimehr, et al. "Analytical modeling of entropy generation for Casson nano-fluid flow induced by a stretching surface." Advanced Powder Technology 26(2): 542-552.

[3] Alkasasbeh, H. (2018). "NUMERICAL SOLUTION ON HEAT TRANSFER MAGNETOHYDRODYNAMIC FLOW OF MICROPOLAR CASSON FLUID OVER A HORIZONTAL CIRCULAR CYLINDER WITH THERMAL RADIATION." Frontiers in Heat and Mass Transfer (FHMT) 10.

[4] Alkasasbeh, H. T., M. Z. Salleh, et al. (2014). "Numerical solutions of radiation effect on magnetohydrodynamic free convection boundary layer flow about a solid sphere with Newtonian heating." Applied Mathematical Sciences 8(140): 6989-7000.

[5] Animasaun, I. L. "Effects of thermophoresis, variable viscosity and thermal conductivity on free convective heat and mass transfer of non-darcian MHD dissipative Casson fluid flow with suction and nth order of chemical reaction." Journal of the Nigerian Mathematical Society 34(1): 11-31.

[6] Ariman, T., M. A. Turk, et al. (1973). "Microcontinuum fluid mechanicsâ€"a review." International Journal of Engineering Science 11(8): 905-930.

[7] Blasius, H. (1908). "Grenzschichten in Flussigkeiten mit kleiner Reibung, 2. angew." Math. Phye 56.

Casson, N. (1959). "A flow equation for pigment-oil suspensions of the printing ink type." Rheology of disperse systems.

[8] Cebeci, T. and P. Bradshaw Physical and computational aspects of convective heat transfer, Springer Science & Business Media.

[9] Cortell Bataller, R. (2008). "Radiation effects in the Blasius flow." Applied mathematics and computation 198(1): 333-338.

[10] Eringen, A. C. (1966). "Theory of micropolar fluids." Journal of Mathematics and Mechanics: 1-18.

[11] Gaffar, S. A., V. R. Prasad, et al. "Magnetohydrodynamic free convection flow and heat transfer of non-Newtonian tangent hyperbolic fluid from horizontal circular cylinder with Biot number effects." International Journal of Applied and Computational Mathematics 3(2): 721-743.

[12] Gul, A. and M. Ullah "Thin Film Flow Analysis of a MHD Third Grade Fluid on a Vertical Belt With no-slip Boundary Conditions." J. Appl. Environ. Biol. Sci 4(10): 71-84.

[13] Haq, R., S. Nadeem, et al. "Convective heat transfer and MHD effects on Casson nanofluid flow over a shrinking sheet." Open Physics 12(12): 862-871.

[14] Ingham, D. B. (1978). "Free-convection boundary layer on an isothermal horizontal cylinder." Zeitschrift fï¼r angewandte Mathematik und Physik ZAMP 29(6): 871-883.

[15] Khalid, A., I. Khan, et al. "Unsteady MHD free convection flow of Casson fluid past over an oscillating vertical plate embedded in a porous medium." Engineering Science and Technology, an International Journal 18(3): 309-317.

[16] Khonsari, M. M. and D. E. Brewe (1994). "Effect of viscous dissipation on the lubrication characteristics of micropolar fluids." Acta Mechanica 105(1-4): 57-68.

[17] Lukaszewicz, G. (1999). Micropolar fluids: theory and applications, Springer Science & Business Media.

[18] Mahdy, A. and S. E. Ahmed "Unsteady MHD convective flow of non-Newtonian Casson fluid in the stagnation region of an impulsively rotating sphere." Journal of Aerospace Engineering 30(5): 04017036.

[19] Malik, M. Y., M. Naseer, et al. "The boundary layer flow of Casson nanofluid over a vertical exponentially stretching cylinder." Applied Nanoscience 4(7): 869-873.

[20] Mehmood, Z., R. Mehmood, et al. "Numerical investigation of micropolar Casson fluid over a stretching sheet with internal heating." Communications in Theoretical Physics 67(4): 443.

[21] Merkin, J. H. (1976). Free convection boundary layer on an isothermal horizontal cylinder. American Society of Mechanical Engineers and American Institute of Chemical Engineers, Heat Transfer Conference, St. Louis, Mo., Aug. 9-11, 1976, ASME 5 p.

[22] Mohammad, N. F. (2015). Magnetohydrodynamic Flow Past a Sphere in a Viscous and Micropolar Fluids for Unsteady Free and Mixed Convective Boundary Layer, Universiti Teknologi Malaysia.

[23] Mukhopadhyay, S., K. Bhattacharyya, et al. "Exact solutions for the flow of Casson fluid over a stretching surface with transpiration and heat transfer effects." Chinese Physics B 22(11): 114701.
[24] Mukhopadhyay, S., K. Bhattacharyya, et al. (2013). "Exact solutions for the flow of Casson fluid over a stretching surface with transpiration and heat transfer effects." Chinese Physics B 22(11): 1-6.
[25] Mukhopadhyay, S., I. C. Mondal, et al. "Casson fluid flow and heat transfer past a symmetric wedge." Heat Transferâ€"Asian Research 42(8): 665-675.
[26] Mustafa, M., T. Hayat, et al. "Unsteady boundary layer flow of a Casson fluid due to an impulsively started moving flat plate." Heat Transferï¼½Asian Research 40(6): 563-576.
[27] Nagendra, N., C. H. Amanulla, et al. "Mathematical Study of Non-Newtonian Nanofluid Transport Phenomena from an Isothermal Sphere." Frontiers in Heat and Mass Transfer (FHMT) 8.
[28] Nazar, R., N. Amin, et al. (2003). "Mixed convection boundary-layer flow from a horizontal circular cylinder in micropolar fluids: case of constant wall temperature." International Journal of Numerical Methods for Heat & Fluid Flow 13(1): 86-109.
[29] Prasad, V. R., A. S. Rao, et al. "Modelling laminar transport phenomena in a Casson rheological fluid from a horizontal circular cylinder with partial slip." Proceedings of the Institution of Mechanical Engineers, Part E: Journal of Process Mechanical Engineering 227(4): 309-326.
[30] Pushpalatha, K., V. Sugunamma, et al. "Heat and mass transfer in unsteady MHD Casson fluid flow with convective boundary conditions." International Journal of Advanced Science and Technology 91: 19-38.
[31] Qasim, M. and S. Noreen "Heat transfer in the boundary layer flow of a Casson fluid over a permeable shrinking sheet with viscous dissipation." The European Physical Journal Plus 129(1): 7.
[32] Shehzad, S. A., T. Hayat, et al. "Effects of mass transfer on MHD flow of Casson fluid with chemical reaction and suction." Brazilian Journal of Chemical Engineering 30(1): 187-195.
[33] Subba Rao, A., V. Ramachandra Prasad, et al. "Heat Transfer in a Casson Rheological Fluid from a Semiâ€ےinfinite Vertical Plate with Partial Slip." Heat Transferâ€"Asian Research 44(3): 272-291.
[34] Swalmeh, M. Z., H. T. Alkasasbeh, et al. (2018). "Heat transfer flow of Cu-water and Al2O3-water micropolar nanofluids about a solid sphere in the presence of natural convection using Keller-box method." Results in Physics 9: 717-724.
[35] Venkatesan, J., D. S. Sankar, et al. "Mathematical analysis of Casson fluid model for blood rheology in stenosed narrow arteries." Journal of Applied Mathematics 2013.